Journal of Computational Mathematics
Vol.33, No.1, 2015, 59–85.

http://www.global-sci.org/jcm
doi:10.4208/jcm.1405-m4368

A CHEBYSHEV-GAUSS SPECTRAL COLLOCATION METHOD FOR ODRINARY DIFFERENTIAL EQUATIONS*

Xi Yang Zhongqing Wang
Department of Mathematics, Shanghai Normal University, Shanghai 200234, China
Scientific Computing Key Laboratory of Shanghai Universities
Division of Computational Science of E-institute of Shanghai Universities
Email: rachel0313@126.com, zqwang@shnu.edu.cn

Abstract

In this paper, we introduce an efficient Chebyshev-Gauss spectral collocation method for initial value problems of ordinary differential equations. We first propose a single interval method and analyze its convergence. We then develop a multi-interval method. The suggested algorithms enjoy spectral accuracy and can be implemented in stable and efficient manners. Some numerical comparisons with some popular methods are given to demonstrate the effectiveness of this approach.

Mathematics subject classification: 65L05, 65L60, 41A10.
Key words: Initial value problems of ordinary differential equations, Chebyshev-Gauss spectral collocation method, Spectral accuracy.

1. Introduction

A considerable amount of literature has been devoted to numerical solutions of ordinary differential equations (ODEs), see, e.g., [6,8,23–25,29,39]. For Hamiltonian systems, the interested reader may refer to [12, 13, 22, 36]. Among the existing methods, numerical schemes based on Taylor's expansions or quadrature formulas have been frequently used, see, e.g., [7,8,23,24,29], which can be systematically designed and often provide accurate approximations.

In the past few decades, spectral method has become increasingly popular and been widely used in spatial discretization of PDEs owing to its spectral accuracy (i.e., the smoother the exact solutions become, the smaller the numerical errors will be), see, e.g., [4,5,9,14–16,37,38]. Moreover, some spectral methods for time discretization of PDEs have been developed rapidly, see, e.g., [2,3,11,27,30,31,40–43]. Recently, Guo et al. [18,19,45] developed several Legendre-Gauss-type spectral collocation methods for ODEs. Meanwhile, Guo et al. [20, 21] designed Laguerre-Gauss-type spectral collocation methods for ODEs. Kanyamee and Zhang [28] also conducted a systematic comparison of a Legendre (Chebyshev)-Gauss-Lobatto spectral collocation method with some symplectic methods in solving Hamiltonian dynamical systems. For the $hp-$version of the continuous Galerkin FEM, we refer the reader to [46] and the references therein for other earlier works.

In this paper, we propose a Chebyshev-Gauss spectral collocation method for ODEs:

$$\begin{cases} \dfrac{d}{dt}U(t) = f(U(t),t), & 0 < t \le T, \\ U(0) = U_0, \end{cases} \tag{1.1}$$

* Received March 4, 2013 / Revised version received April 14, 2014 / Accepted May 26, 2014 / Published online December 1, 2014 /

where f is a given function, and U_0 is the initial data.

We start with a single interval scheme. We approximate the solution by a finite Chebyshev series, and collocate the numerical scheme at Chebyshev-Gauss points to determine the coefficients. We introduce two algorithms. Numerical results show that the suggested algorithms can be implemented efficiently. Particularly, the algorithms are numerically stable and possess spectral accuracy. It is noted that Vigo-Aguiar and Ramos [44] also constructed a special family of Runge-Kutta collocation algorithms based on Chebyshev-Gauss-Lobatto points, with A-stability and stiffly accurate characteristics. The interested reader may also refer to [34, 35] for additional information.

For a more effective implementation, we also suggest a multi-interval scheme due to the following considerations:

- The resultant system for the expansion coefficients can be solved more efficiently for a modest number of unknowns. For large T, it is desirable to partition the solution interval $(0, T)$ and solve the subsystems successively. Hence, the scheme can be implemented efficiently and economically.

- For ensuring the convergence of the numerical scheme, the length of T is limited sometimes.

- The multi-interval scheme provides us sufficient flexibility to handle ODEs, e.g., we may use geometrically refined steps and linearly increasing degree vectors to resolve the singular behavior of the solution.

Numerical illustrations also show that the suggested algorithms are particularly attractive for ODEs with stiff behaviors, oscillating solutions, steep gradient solutions and long time calculations.

We highlight the main differences between our strategy and the existing ones as follows.

- We collocate the numerical scheme at Chebyshev-Gauss points, and analyze the convergence of the single interval scheme. The nodes and weights of Chebyshev-Gauss quadratures are given explicitly, avoiding the potential loss of accuracy (compared with Legendre and Laguerre quadratures). Particularly, the algorithm can be implemented efficiently by using fast Chebyshev transform. The existing work on spectral collocation methods [18–21, 45] studied the Legendre and Laguerre collocation schemes.

- We use the Chebyshev expansions in each sub-step (known to be much stable than the usual Lagrange approach [38]), which lead to quite neat implementation through manipulating the expansion coefficients (see (2.24) below). The existing work on spectral collocation methods [18–21, 45] considered the Legendre and Laguerre expansions in each sub-step, but did not establish the relationships of the expansion coefficients.

The paper is organized as follows. In the next section, we present and analyze the single interval Chebyshev-Gauss collocation method, and provide some numerical results to justify our theoretical analysis. In Section 3, we describe the multi-interval Chebyshev-Gauss collocation method, the convergence is illustrated numerically. The final section is for some concluding discussions.

We end this section with some notations to be used throughout the paper:

- For a given interval Λ and a certain weight function χ, we denote by $H^r_\chi(\Lambda)$, $r \geq 0$ the weighted Sobolev space in the usual way. In particular, $H^0_\chi(\Lambda) = L^2_\chi(\Lambda)$.
- For simplicity, we sometimes denote $\frac{d}{dt}v(t) = v'(t)$.

2. Single Interval Chebyshev-Gauss Collocation Method

In this section, we describe and analyze a single interval Chebyshev-Gauss numerical integration process for the ordinary differential equations. We also present some numerical results to illustrate the efficiency.

2.1. Preliminaries

Let $\mathcal{T}_l(x),\ x \in [-1,1]$ be the standard Chebyshev polynomial of degree l. We recall that $\mathcal{T}_l(x)$ is the eigenfunction of the singular Sturm-Liouville problem

$$(1-x^2)y''(x) - xy'(x) + l^2 y(x) = 0, \quad l = 0, 1, \cdots. \tag{2.1}$$

We define the shifted Chebyshev polynomials $\mathcal{T}_{T,l}(t)$ by

$$\mathcal{T}_{T,l}(t) = \mathcal{T}_l\left(\frac{2t}{T} - 1\right), \quad t \in [0,T], \quad l = 0, 1 \cdots.$$

In particular,

$$\mathcal{T}_{T,0}(t) = 1, \qquad \mathcal{T}_{T,1}(t) = \frac{2t}{T} - 1, \qquad \mathcal{T}_{T,2}(t) = \frac{8t^2}{T^2} - \frac{8t}{T} + 1. \tag{2.2}$$

According to the properties of the standard Chebyshev polynomials, we have

$$\mathcal{T}_{T,l+1}(t) - 2\left(\frac{2t}{T} - 1\right)\mathcal{T}_{T,l}(t) + \mathcal{T}_{T,l-1}(t) = 0, \qquad l \geq 1, \tag{2.3}$$

$$\frac{1}{l+1}\mathcal{T}'_{T,l+1}(t) - \frac{1}{l-1}\mathcal{T}'_{T,l-1}(t) = \frac{4}{T}\mathcal{T}_{T,l}(t), \qquad l \geq 2. \tag{2.4}$$

Let $\omega(t) = t(T-t)$. The set of $\mathcal{T}_{T,l}(t)$ forms a complete $L^2_{\omega^{-1/2}}(0,T)-$orthogonal system,

$$\int_0^T \mathcal{T}_{T,l}(t)\mathcal{T}_{T,m}(t)\omega^{-\frac{1}{2}}(t)dt = \frac{1}{2}\pi c_l \delta_{l,m}, \tag{2.5}$$

where $c_0 = 2$, $c_l = 1$ for $l \geq 1$ and $\delta_{l,m}$ is the Kronecker symbol. Thus for any $v(t) \in L^2_{\omega^{-1/2}}(0,T)$, we can write

$$v(t) = \sum_{l=0}^{\infty} \widehat{v}_l \mathcal{T}_{T,l}(t), \qquad \widehat{v}_l = \frac{2}{\pi c_l}\int_0^T v(t)\mathcal{T}_{T,l}(t)\omega^{-\frac{1}{2}}(t)dt. \tag{2.6}$$

Moreover, by (2.1) we can verify readily that

$$\int_0^T \mathcal{T}'_{T,l}(t)\mathcal{T}'_{T,m}(t)\omega^{\frac{1}{2}}(t)dt = \frac{\pi}{2}l^2 c_l \delta_{l,m}. \tag{2.7}$$

We now deal with the shifted Chebyshev-Gauss interpolation. We denote

$$x_j^N = -\cos\frac{(2j+1)\pi}{2N+2}, \quad 0 \leq j \leq N,$$

which are the standard Chebyshev-Gauss points on the interval $(-1,1)$, and

$$t_{T,j}^N = \frac{T}{2}(x_j^N + 1) = \frac{T}{2}\left(1 - \cos\frac{(2j+1)\pi}{2N+2}\right), \quad 0 \le j \le N.$$

Clearly, $t_{T,j}^N,\ 0 \le j \le N$ are the zeros of $\mathcal{T}_{T,N+1}(t)$.

Let $\mathcal{P}_N(0,T)$ be the set of polynomials of degree at most N. The standard Chebyshev-Gauss formula implies that for any $\phi \in \mathcal{P}_{2N+1}(0,T)$,

$$\begin{aligned}\int_0^T \phi(t)\omega^{-\frac{1}{2}}(t)dt &= \int_{-1}^1 \phi(\frac{T}{2}(x+1))(1-x^2)^{-\frac{1}{2}}dx \\ &= \frac{\pi}{N+1}\sum_{j=0}^N \phi(\frac{T}{2}(x_j^N+1)) = \frac{\pi}{N+1}\sum_{j=0}^N \phi(t_{T,j}^N). \end{aligned} \tag{2.8}$$

Next denote by $(u,v)_{T,\omega}$ and $\|v\|_{T,\omega}$ the inner product and norm of the space $L^2_{\omega^{-1/2}}(0,T)$, respectively,

$$(u,v)_{T,\omega} = \int_0^T u(t)v(t)\omega^{-\frac{1}{2}}(t)dt, \qquad \|v\|_{T,\omega} = (v,v)_{T,\omega}^{\frac{1}{2}}.$$

The discrete inner product and the discrete norm associated with the shifted Chebyshev-Gauss interpolation points are,

$$(u,v)_{T,N} = \frac{\pi}{N+1}\sum_{j=0}^N u(t_{T,j}^N)v(t_{T,j}^N), \qquad \|v\|_{T,N} = (v,v)_{T,N}^{\frac{1}{2}}.$$

Thanks to (2.8), for any $\phi\psi \in \mathcal{P}_{2N+1}(0,T)$ and $\varphi \in \mathcal{P}_N(0,T)$, we have

$$(\phi,\psi)_{T,\omega} = (\phi,\psi)_{T,N}, \qquad \|\varphi\|_{T,\omega} = \|\varphi\|_{T,N}. \tag{2.9}$$

The shifted Chebyshev-Gauss interpolation operator $\mathcal{I}_{T,N}v(t) : C(0,T) \to \mathcal{P}_N(0,T)$ is such that

$$\mathcal{I}_{T,N}v(t_{T,j}^N) = v(t_{T,j}^N), \qquad 0 \le j \le N.$$

Because of (2.9), we obtain that for any $\phi \in \mathcal{P}_{N+1}(0,T)$,

$$(\mathcal{I}_{T,N}v,\phi)_{T,\omega} = (\mathcal{I}_{T,N}v,\phi)_{T,N} = (v,\phi)_{T,N}. \tag{2.10}$$

We can expand $\mathcal{I}_{T,N}v(t)$ as

$$\mathcal{I}_{T,N}v(t) = \sum_{l=0}^N \widetilde{v}_l \mathcal{T}_{T,l}(t). \tag{2.11}$$

Using (2.5) and (2.10) yields

$$\widetilde{v}_l = \frac{2}{\pi c_l}(\mathcal{I}_{T,N}v, \mathcal{T}_{T,l})_{T,\omega} = \frac{2}{\pi c_l}(v, \mathcal{T}_{T,l})_{T,N}, \qquad 0 \le l \le N. \tag{2.12}$$

Next, for any $\psi \in \mathcal{P}_{N+1}(0,T)$, we write

$$\psi(t) = \sum_{l=0}^{N+1} \widehat{\psi}_l \mathcal{T}_{T,l}(t) \qquad \text{and} \qquad \mathcal{I}_{T,N}\psi(t) = \sum_{l=0}^N \widetilde{\psi}_l \mathcal{T}_{T,l}(t). \tag{2.13}$$

With the aid of (2.12), (2.9) and (2.6), we deduce that

$$\widetilde{\psi}_l = \frac{2}{\pi c_l}(\psi, \mathcal{T}_{T,l})_{T,N} = \frac{2}{\pi c_l}(\psi, \mathcal{T}_{T,l})_{T,\omega} = \widehat{\psi}_l, \qquad 0 \le l \le N. \tag{2.14}$$

The above result, along with (2.5) and (2.10), gives that

$$\begin{aligned} \|\psi\|^2_{T,N} &= \|\mathcal{I}_{T,N}\psi\|^2_{T,N} = \|\mathcal{I}_{T,N}\psi\|^2_{T,\omega} = \sum_{l=0}^{N} \frac{1}{2}\pi c_l \widetilde{\psi}_l^2 \\ &= \sum_{l=0}^{N} \frac{1}{2}\pi c_l \widehat{\psi}_l^2 \le \sum_{l=0}^{N+1} \frac{1}{2}\pi c_l \widehat{\psi}_l^2 = \|\psi\|^2_{T,\omega}, \qquad \forall \psi \in \mathcal{P}_{N+1}(0,T). \end{aligned} \tag{2.15}$$

2.2. The single interval scheme

The single interval collocation scheme for solving (1.1) is to seek $u^N(t) \in \mathcal{P}_{N+1}(0,T)$ such that

$$\begin{cases} \dfrac{d}{dt}u^N(t^N_{T,j}) = f(u^N(t^N_{T,j}), t^N_{T,j}), & 0 \le j \le N, \\ u^N(0) = U_0. \end{cases} \tag{2.16}$$

The following proposition, proven in Appendix A, shows that if $f(z,t)$ fulfills the Lipschitz condition:

$$|f(z_1,t) - f(z_2,t)| \le \gamma |z_1 - z_2|, \quad \gamma > 0, \tag{2.17}$$

then the system (2.16) is uniquely solvable, as long as the time step T is sufficiently small.

Proposition 2.1. *Assume that $f(z,t)$ fulfills the Lipschitz condition* (2.17)*, and*

$$0 < \gamma T \le \beta < \frac{1}{4}, \tag{2.18}$$

where β is a certain constant. Then the method (2.16) *admits a unique solution.*

We now describe the numerical implementations and present some algorithms for scheme (2.16). According to (2.16), we get that

$$\frac{d}{dt}u^N(t) = \mathcal{I}_{T,N} f(u^N(t), t). \tag{2.19}$$

Next, let

$$u^N(t) = \sum_{k=0}^{N+1} \widehat{u}_k \mathcal{T}_{T,k}(t), \tag{2.20}$$

$$\mathcal{I}_{T,N} f(u^N(t), t) = \sum_{k=0}^{N} \widehat{f}_k \mathcal{T}_{T,k}(t). \tag{2.21}$$

Due to (2.5) and (2.9), we get that

$$\begin{aligned} \widehat{f}_k &= \frac{2}{\pi c_k}(\mathcal{I}_{T,N} f(u^N, \cdot), \mathcal{T}_{T,k})_{T,\omega} = \frac{2}{\pi c_k}(\mathcal{I}_{T,N} f(u^N, \cdot), \mathcal{T}_{T,k})_{T,N} \\ &= \frac{2}{c_k(N+1)} \sum_{j=0}^{N} f(u^N(t^N_{T,j}), t^N_{T,j}) \mathcal{T}_{T,k}(t^N_{T,j}), \qquad \forall 0 \le k \le N. \end{aligned} \tag{2.22}$$

Moreover, by (2.19)-(2.21), (2.4) and (2.2), we derive that

$$\begin{aligned}
\sum_{k=1}^{N+1}\widehat{u}_k\mathcal{T}'_{T,k}(t) =&\sum_{k=0}^{N}\widehat{f}_k\mathcal{T}_{T,k}(t)\\
=&\widehat{f}_0+\widehat{f}_1\mathcal{T}_{T,1}(t)+\sum_{k=2}^{N}\widehat{f}_k\mathcal{T}_{T,k}(t)\\
=&\widehat{f}_0+\widehat{f}_1\mathcal{T}_{T,1}(t)+\frac{T}{4}\sum_{k=2}^{N}\frac{\widehat{f}_k}{k+1}\mathcal{T}'_{T,k+1}(t)-\frac{T}{4}\sum_{k=2}^{N}\frac{\widehat{f}_k}{k-1}\mathcal{T}'_{T,k-1}(t)\\
=&\frac{T\widehat{f}_N}{4(N+1)}\mathcal{T}'_{T,N+1}(t)+\frac{T\widehat{f}_{N-1}}{4N}\mathcal{T}'_{T,N}(t)+\frac{T}{4}\sum_{k=3}^{N-1}\frac{\widehat{f}_{k-1}}{k}\mathcal{T}'_{T,k}(t)\\
&-\frac{T}{4}\sum_{k=1}^{N-1}\frac{\widehat{f}_{k+1}}{k}\mathcal{T}'_{T,k}(t)+\widehat{f}_1\mathcal{T}_{T,1}(t)+\widehat{f}_0\\
=&\frac{T\widehat{f}_N}{4(N+1)}\mathcal{T}'_{T,N+1}(t)+\frac{T\widehat{f}_{N-1}}{4N}\mathcal{T}'_{T,N}(t)+\frac{T}{4}\sum_{k=3}^{N-1}\frac{\widehat{f}_{k-1}-\widehat{f}_{k+1}}{k}\mathcal{T}'_{T,k}(t)\\
&-\frac{T\widehat{f}_3}{8}\mathcal{T}'_{T,2}(t)-\frac{T\widehat{f}_2}{4}\mathcal{T}'_{T,1}(t)+\widehat{f}_1\mathcal{T}_{T,1}(t)+\widehat{f}_0\\
=&\frac{T\widehat{f}_N}{4(N+1)}\mathcal{T}'_{T,N+1}(t)+\frac{T\widehat{f}_{N-1}}{4N}\mathcal{T}'_{T,N}(t)+\frac{T}{4}\sum_{k=1}^{N-1}\frac{c_{k-1}\widehat{f}_{k-1}-\widehat{f}_{k+1}}{k}\mathcal{T}'_{T,k}(t).
\end{aligned}\tag{2.23}$$

Since $\{\mathcal{T}'_{T,k}(t)\}$ are mutually orthogonal with respect to the weight $\omega^{\frac{1}{2}}(t)$ (see (2.7)), we can compare the expansion coefficients in terms of $\mathcal{T}'_{T,k}(t)$ to obtain that

$$\begin{aligned}
&\widehat{u}_{N+1}=\frac{T\widehat{f}_N}{4(N+1)},\qquad \widehat{u}_N=\frac{T\widehat{f}_{N-1}}{4N},\\
&\widehat{u}_k=\frac{T(c_{k-1}\widehat{f}_{k-1}-\widehat{f}_{k+1})}{4k},\qquad 1\le k\le N-1.
\end{aligned}\tag{2.24}$$

On the other hand, $\mathcal{T}_{T,k}(0)=(-1)^k$. Hence by taking $t=0$ in (2.20) and using (2.16), we get that

$$\widehat{u}_0=U_0+\sum_{k=1}^{N+1}(-1)^{k-1}\widehat{u}_k.\tag{2.25}$$

In actual computation, an iterative process can be employed to evaluate the values $\{u^N(t^N_{T,i})\}_{i=0}^N$or the expansion coefficients $\{\widehat{u}_k\}_{k=0}^{N+1}$, as stated below.

(i). The Newton iterative method. By (2.20), (2.25) and (2.24) we obtain that

$$\begin{aligned}
u^N(t)=&\sum_{k=0}^{N+1}\widehat{u}_k\mathcal{T}_{T,k}(t)=U_0+\sum_{k=1}^{N+1}\widehat{u}_k(\mathcal{T}_{T,k}(t)+(-1)^{k-1})\\
=&U_0+\frac{T\widehat{f}_N}{4(N+1)}(\mathcal{T}_{T,N+1}(t)+(-1)^N)+\frac{T\widehat{f}_{N-1}}{4N}(\mathcal{T}_{T,N}(t)+(-1)^{N-1})\\
&+\sum_{k=1}^{N-1}\frac{T(c_{k-1}\widehat{f}_{k-1}-\widehat{f}_{k+1})}{4k}(\mathcal{T}_{T,k}(t)+(-1)^{k-1}).
\end{aligned}\tag{2.26}$$

A combination of (2.26) and (2.22) yields

$$u^N(t) = F(u^N, t), \tag{2.27}$$

where

$$\begin{aligned}
F(u^N,t) &= U_0 + \frac{T}{2(N+1)^2}\Big(\mathcal{T}_{T,N+1}(t) + (-1)^N\Big)\sum_{j=0}^{N} f(u^N(t_{T,j}^N), t_{T,j}^N)\mathcal{T}_{T,N}(t_{T,j}^N)\\
&+\frac{T}{2N(N+1)}\Big(\mathcal{T}_{T,N}(t) + (-1)^{N-1}\Big)\sum_{j=0}^{N} f(u^N(t_{T,j}^N), t_{T,j}^N)\mathcal{T}_{T,N-1}(t_{T,j}^N)\\
&+\sum_{k=1}^{N-1}\frac{T}{2k(N+1)}\Big(\mathcal{T}_{T,k}(t) + (-1)^{k-1}\Big)\sum_{j=0}^{N} f(u^N(t_{T,j}^N), t_{T,j}^N)\Big(\mathcal{T}_{T,k-1}(t_{T,j}^N) - \mathcal{T}_{T,k+1}(t_{T,j}^N)\Big).
\end{aligned}$$

Thus, we may evaluate the values $\{u^N(t_{T,i}^N)\}_{i=0}^N$ by using the Newton iterative process.

Next, for any $0 \le l \le N$, we have $u^N(t)\mathcal{T}_{T,l}(t) \in \mathcal{P}_{2N+1}(0,T)$. Therefore, multiplying (2.20) by $\omega^{-\frac{1}{2}}(t)\mathcal{T}_{T,l}(t)$, integrating the result over the interval $(0,T)$, and using (2.5) and (2.9), we verify readily that

$$\begin{aligned}
\widehat{u}_l &= \frac{2}{\pi c_l}(u^N, \mathcal{T}_{T,l})_{T,\omega} = \frac{2}{\pi c_l}(u^N, \mathcal{T}_{T,l})_{T,N}\\
&= \frac{2}{c_l(N+1)}\sum_{j=0}^{N} u^N(t_{T,j}^N)\mathcal{T}_{T,l}(t_{T,j}^N), \quad 0 \le l \le N.
\end{aligned} \tag{2.28}$$

On the other hand, $\mathcal{T}_{T,l}(0) = (-1)^l$. Hence by taking $t = 0$ in (2.20), we obtain from (2.28) that

$$\begin{aligned}
\widehat{u}_{N+1} &= (-1)^{N+1}U_0 + \sum_{l=0}^{N}(-1)^{N+l}\widehat{u}_l\\
&= (-1)^{N+1}U_0 + \frac{2}{N+1}\sum_{l=0}^{N}(-1)^{N+l}c_l^{-1}\sum_{j=0}^{N} u^N(t_{T,j}^N)\mathcal{T}_{T,l}(t_{T,j}^N).
\end{aligned} \tag{2.29}$$

Finally, by using (2.20), (2.28), (2.29), we obtain

$$\begin{aligned}
u^N(T) &= \sum_{l=0}^{N+1}\widehat{u}_l\\
&= \frac{2}{N+1}\sum_{l=0}^{N} c_l^{-1}(1+(-1)^{N+l})\sum_{j=0}^{N} u^N(t_{T,j}^N)\mathcal{T}_{T,l}(t_{T,j}^N) + (-1)^{N+1}U_0.
\end{aligned} \tag{2.30}$$

(ii). The simple iterative method. We may use a simple iterative algorithm (also called successive substitution method) presented in Algorithm (2.1) to evaluate the expansion coefficients $\{\widehat{u}_k\}_{k=0}^{N+1}$.

Algorithm 2.1: The simple iterative algorithm.

Step 1. Provide the initial guess of $u^N(t)$ at the collocation points $\{t_{T,j}^N\}_{j=0}^N$;

Step 2. Evaluate the values of $f(u^N(t_{T,j}^N), t_{T,j}^N), \qquad 0 \le j \le N$;

Step 3. Compute the coefficients $\{\widehat{f}_k\}_{k=0}^N$ by (2.22);

Step 4. Compute the coefficients $\{\widehat{u}_k\}_{k=0}^{N+1}$ by (2.24) and (2.25);

Step 5. Update the data of $u^N(t)$ at the collocation points $\{t_{T,j}^N\}_{j=0}^N$ by (2.20);

Step 6. Repeat Steps 2-5 until the maximum of the absolute difference between two consecutive values of $\{u^N(t_{T,j}^N)\}_{j=0}^N$ is less than the desired tolerance;

Step 7. Compute $u^N(T) = \sum_{k=0}^{N+1} \widehat{u}_k$ by (2.20).

The simple iterative algorithm has the following attractive advantages:

- It is much simpler and easier to design codes;
- We do not require to solve in each iteration a linear system of equations;
- The discrete Chebyshev transform (treated as a Fourier-cosine transform) can be performed.

2.3. Error analysis

In this subsection, we shall analyze the numerical error of the single interval scheme (2.16). As usual, we first compare $u^N(t)$ with the interpolation $\mathcal{I}_{T,N}U(t)$. For this purpose, let

$$G_{T,1}^N(t) = \mathcal{I}_{T,N}\frac{d}{dt}U(t) - \frac{d}{dt}\mathcal{I}_{T,N}U(t).$$

Then we have from (1.1) that

$$\frac{d}{dt}\mathcal{I}_{T,N}U(t_{T,k}^N) = f(U(t_{T,k}^N), t_{T,k}^N) - G_{T,1}^N(t_{T,k}^N), \qquad 0 \le k \le N. \tag{2.31}$$

Further, let $E^N(t) = u^N(t) - \mathcal{I}_{T,N}U(t)$. Subtracting (2.31) from (2.16) yields

$$\begin{cases} \dfrac{d}{dt}E^N(t_{T,k}^N) = G_{T,1}^N(t_{T,k}^N) + G_{T,2}^N(t_{T,k}^N), & 0 \le k \le N, \\ E^N(0) = U_0 - \mathcal{I}_{T,N}U(0), \end{cases} \tag{2.32}$$

where

$$G_{T,2}^N(t_{T,k}^N) = f(u^N(t_{T,k}^N), t_{T,k}^N) - f(\mathcal{I}_{T,N}U(t_{T,k}^N), t_{T,k}^N).$$

For simplicity, we denote $R_N(t) = t^{-1}(E^N(t) - E^N(0))$. Clearly $R_N(t) \in \mathcal{P}_N(0,T)$. Hence

by integrating by parts, we deduce that

$$\begin{aligned}
&2((T-t)R_N, \frac{d}{dt}(tR_N))_{T,N} = 2((T-t)R_N, \frac{d}{dt}(tR_N))_{T,\omega}\\
&= 2\int_0^T R_N^2(t)\frac{T-t}{\sqrt{t(T-t)}}dt + 2\int_0^T R_N(t)\frac{d}{dt}R_N(t)\sqrt{t(T-t)}dt\\
&= 2\int_0^T R_N^2(t)\frac{T-t}{\sqrt{t(T-t)}}dt + R_N^2(t)\sqrt{t(T-t)}\Big|_0^T - \int_0^T R_N^2(t)\frac{T-2t}{2\sqrt{t(T-t)}}dt\\
&= \int_0^T R_N^2(t)\frac{1}{\sqrt{t(T-t)}}(\frac{3}{2}T-t)dt \geq \frac{T}{2}\|R_N\|^2_{T,\omega}. \qquad (2.33)
\end{aligned}$$

On the other hand, by virtue of (2.32), we get that

$$\begin{aligned}
&2((T-t)R_N, \frac{d}{dt}(tR_N))_{T,N} = 2((T-t)R_N, \frac{d}{dt}(E^N - E^N(0)))_{T,N}\\
&= 2((T-t)R_N, G^N_{T,1} + G^N_{T,2})_{T,N} = A^N_{T,1} + A^N_{T,2}, \qquad (2.34)
\end{aligned}$$

where

$$A^N_{T,1} = 2((T-t)R_N, G^N_{T,1})_{T,N}, \quad A^N_{T,2} = 2((T-t)R_N, G^N_{T,2})_{T,N}.$$

Moreover, due to (2.15), we obtain that for any $\varepsilon > 0$,

$$\begin{aligned}
|A^N_{T,1}| &\leq 2\|(T-t)R_N\|_{T,N}\|G^N_{T,1}\|_{T,N} \leq 2\|(T-t)R_N\|_{T,\omega}\|G^N_{T,1}\|_{T,\omega}\\
&\leq \frac{\varepsilon}{T}\|(T-t)R_N\|^2_{T,\omega} + \varepsilon^{-1}T\|G^N_{T,1}\|^2_{T,\omega}\\
&\leq \varepsilon T\|t^{-1}(E^N - E^N(0))\|^2_{T,\omega} + \varepsilon^{-1}T\|G^N_{T,1}\|^2_{T,\omega}. \qquad (2.35)
\end{aligned}$$

Therefore, we derive from (2.33)-(2.35) that

$$\Big(\frac{1}{2} - \varepsilon\Big)T\|t^{-1}(E^N - E^N(0))\|^2_{T,\omega} \leq \varepsilon^{-1}T\|G^N_{T,1}\|^2_{T,\omega} + A^N_{T,2}. \qquad (2.36)$$

We next estimate $\|G^N_{T,1}\|_{T,\omega}$. Let $\chi(x) = 1 - x^2$ and $\mathcal{I}_N$ be the standard Chebyshev-Gauss interpolation on the interval $(-1, 1)$. Denote by c a generic positive constant independent of T, N and any function. According to (4.24) of [17] with $\alpha = \beta = \gamma = \delta = -\frac{1}{2}$, for any $v \in H^r_{\chi^{r-\frac{1}{2}}}(-1, 1)$ and integer $1 \leq r \leq N+1$,

$$\|\mathcal{I}_N v - v\|^2_{L^2_{\chi^{-\frac{1}{2}}}(-1,1)} \leq cN^{-2r}\int_{-1}^1 \chi^{r-\frac{1}{2}}(x)\Big(\frac{d^r}{dx^r}v(x)\Big)^2 dx. \qquad (2.37)$$

Moreover, by (4.25) of [17] with $\alpha = \beta = -\frac{1}{2}$, for any $v \in H^r_{\chi^{r-\frac{3}{2}}}(-1, 1)$ and integer $2 \leq r \leq N+1$,

$$\Big\|\frac{d}{dx}(\mathcal{I}_N v - v)\Big\|^2_{L^2_{\chi^{-\frac{1}{2}}}(-1,1)} \leq cN^{4-2r}\int_{-1}^1 \chi^{r-\frac{3}{2}}(x)\Big(\frac{d^r}{dx^r}v(x)\Big)^2 dx. \qquad (2.38)$$

Accordingly,

$$\|\mathcal{I}_{T,N} v - v\|^2_{T,\omega} \leq cN^{-2r}\int_0^T \omega^{r-\frac{1}{2}}(t)\Big(\frac{d^r}{dt^r}v(t)\Big)^2 dt, \qquad (2.39)$$

$$\Big\|\frac{d}{dt}(\mathcal{I}_{T,N} v - v)\Big\|^2_{T,\omega} \leq cN^{4-2r}\int_0^T \omega^{r-\frac{3}{2}}(t)\Big(\frac{d^r}{dt^r}v(t)\Big)^2 dt. \qquad (2.40)$$

Hence by (2.39) with $\frac{dU}{dt}$ and $r-1$, instead of v and r, we have that for integer $2 \le r \le N+2$,

$$\left\|\mathcal{I}_{T,N}\frac{d}{dt}U - \frac{d}{dt}U\right\|_{T,\omega}^2 \le cN^{2-2r}\int_0^T \omega^{r-\frac{3}{2}}(t)\left(\frac{d^r}{dt^r}U(t)\right)^2 dt. \tag{2.41}$$

The above with (2.40) gives that for integer $2 \le r \le N+1$,

$$\begin{aligned}\|G_{T,1}^N\|_{T,\omega}^2 &\le 2\left\|\frac{d}{dt}(\mathcal{I}_{T,N}U - U)\right\|_{T,\omega}^2 + 2\left\|\mathcal{I}_{T,N}\frac{d}{dt}U - \frac{d}{dt}U\right\|_{T,\omega}^2 \\ &\le cN^{4-2r}\int_0^T \omega^{r-\frac{3}{2}}(t)\left(\frac{d^r}{dt^r}U(t)\right)^2 dt.\end{aligned} \tag{2.42}$$

Substituting (2.42) into (2.36), we obtain that

$$\begin{aligned}&\left(\frac{1}{2}-\varepsilon\right)T\|t^{-1}(E^N - E^N(0))\|_{T,\omega}^2 \\ &\le A_{T,2}^N + c\varepsilon^{-1}TN^{4-2r}\int_0^T \omega^{r-\frac{3}{2}}(t)\left(\frac{d^r}{dt^r}U(t)\right)^2 dt.\end{aligned} \tag{2.43}$$

Theorem 2.1. *Assume that $f(z,t)$ fulfills the Lipschitz condition* (2.17)*, and* (2.18) *holds. Then for any $U \in H^r_{\omega^{r-\frac{3}{2}}}(0,T)$ with integers $2 \le r \le N+1$, we have*

$$\|U - u^N\|_{L^2(0,T)}^2 \le \frac{T}{2}\|U - u^N\|_{T,\omega}^2 \le c_\beta T^3 N^{4-2r}\int_0^T \omega^{r-\frac{3}{2}}(t)\left(\frac{d^r}{dt^r}U(t)\right)^2 dt, \tag{2.44}$$

$$|U(T) - u^N(T)|^2 \le c_\beta T^2 N^{4-2r}\int_0^T \omega^{r-\frac{3}{2}}(t)\left(\frac{d^r}{dt^r}U(t)\right)^2 dt, \tag{2.45}$$

where c_β is a positive constant depending only on β.

Proof. By (2.17) and (2.15), we deduce that

$$\begin{aligned}\|G_{T,2}^N\|_{T,N}^2 &= \frac{\pi}{N+1}\sum_{j=0}^N |f(u^N(t_{T,j}^N), t_{T,j}^N) - f(\mathcal{I}_{T,N}(U(t_{T,j}^N), t_{T,j}^N)|^2 \\ &\le \frac{\pi\gamma^2}{N+1}\sum_{j=0}^N |u^N(t_{T,j}^N) - \mathcal{I}_{T,N}U(t_{T,j}^N)|^2 = \gamma^2\|u^N - \mathcal{I}_{T,N}U\|_{T,N}^2 \\ &\le \gamma^2\|u^N - \mathcal{I}_{T,N}U\|_{T,\omega}^2 = \gamma^2\|E^N\|_{T,\omega}^2.\end{aligned} \tag{2.46}$$

The above with (2.15) gives that

$$\begin{aligned}A_{T,2}^N &\le \gamma\|(T-t)R_N\|_{T,N}^2 + \gamma^{-1}\|G_{T,2}^N\|_{T,N}^2 \\ &\le \gamma\|(T-t)R_N\|_{T,\omega}^2 + \gamma\|E^N\|_{T,\omega}^2 \\ &\le \gamma T^2\|t^{-1}(E^N - E^N(0))\|_{T,\omega}^2 + \gamma\|E^N\|_{T,\omega}^2.\end{aligned} \tag{2.47}$$

Substituting (2.47) into (2.43), we derive that

$$\begin{aligned}&\left(\frac{1}{2}-\varepsilon-\gamma T\right)T\|t^{-1}(E^N - E^N(0))\|_{T,\omega}^2 \\ &\le \gamma\|E^N\|_{T,\omega}^2 + c\varepsilon^{-1}TN^{4-2r}\int_0^T \omega^{r-\frac{3}{2}}(t)\left(\frac{d^r}{dt^r}U(t)\right)^2 dt.\end{aligned} \tag{2.48}$$

Moreover, a direct calculation shows that

$$\begin{aligned}\|E^N\|^2_{T,\omega} &\le (1+\varepsilon)\|E^N - E^N(0)\|^2_{T,\omega} + (1+\varepsilon^{-1})\|E^N(0)\|^2_{T,\omega}\\ &\le (1+\varepsilon)T^2\|t^{-1}(E^N - E^N(0))\|^2_{T,\omega} + \pi(1+\varepsilon^{-1})|E^N(0)|^2. \end{aligned} \tag{2.49}$$

Therefore, by (2.48) and (2.49) we get

$$\begin{aligned}&\Big(\frac{1}{2} - \varepsilon - \gamma T\Big)T\|E^N\|^2_{T,\omega}\\ \le&(1+\varepsilon)T^2\bigg(\gamma\|E^N\|^2_{T,\omega} + c\varepsilon^{-1}TN^{4-2r}\int_0^T \omega^{r-\frac{3}{2}}(t)\Big(\frac{d^r}{dt^r}U(t)\Big)^2dt\bigg)\\ &+\pi(1+\varepsilon^{-1})\Big(\frac{1}{2} - \varepsilon - \gamma T\Big)T|E^N(0)|^2,\end{aligned} \tag{2.50}$$

or equivalently,

$$\begin{aligned}&\Big(\frac{1}{2} - \varepsilon - 2\gamma T - \varepsilon\gamma T\Big)\|E^N\|^2_{T,\omega}\\ \le& c\varepsilon^{-1}T^2N^{4-2r}\int_0^T \omega^{r-\frac{3}{2}}(t)\Big(\frac{d^r}{dt^r}U(t)\Big)^2dt + \pi(1+\varepsilon^{-1})\Big(\frac{1}{2} - \varepsilon - \gamma T\Big)|E^N(0)|^2.\end{aligned} \tag{2.51}$$

On the other hand, for any $v \in H^1_{\omega^{-\frac{1}{2}}}(0,T)$ (see Appendix B of this paper),

$$\max_{t\in[0,T]}|v(t)|^2 \le \frac{\pi}{4}\Big(\|v\|^2_{T,\omega} + T^2\|\frac{dv}{dt}\|^2_{T,\omega}\Big). \tag{2.52}$$

A combination of (2.39), (2.40) and (2.52) leads to

$$\begin{aligned}|E^N(0)|^2 = |\mathcal{I}_{T,N}U(0) - U(0)|^2 &\le \frac{\pi}{4}\Big(\|\mathcal{I}_{T,N}U - U\|^2_{T,\omega} + T^2\|\frac{d}{dt}(\mathcal{I}_{T,N}U - U)\|^2_{T,\omega}\Big)\\ &\le cN^{-2r}\int_0^T \omega^{r-\frac{1}{2}}(t)\Big(\frac{d^r}{dt^r}U(t)\Big)^2dt + cT^2N^{4-2r}\int_0^T \omega^{r-\frac{3}{2}}(t)\Big(\frac{d^r}{dt^r}U(t)\Big)^2dt\\ &\le cT^2N^{-2r}\int_0^T \omega^{r-\frac{3}{2}}(t)\Big(\frac{d^r}{dt^r}U(t)\Big)^2dt + cT^2N^{4-2r}\int_0^T \omega^{r-\frac{3}{2}}(t)\Big(\frac{d^r}{dt^r}U(t)\Big)^2dt\\ &\le cT^2N^{4-2r}\int_0^T \omega^{r-\frac{3}{2}}(t)\Big(\frac{d^r}{dt^r}U(t)\Big)^2dt.\end{aligned} \tag{2.53}$$

Substituting (2.53) into (2.51), we observe that

$$\Big(\frac{1}{2} - \varepsilon - 2\gamma T - \varepsilon\gamma T\Big)\|E^N\|^2_{T,\omega} \le c\varepsilon^{-1}T^2N^{4-2r}\int_0^T \omega^{r-\frac{3}{2}}\Big(\frac{d^r}{dt^r}U(t)\Big)^2dt. \tag{2.54}$$

Take $\varepsilon = \frac{\frac{1}{4}-\gamma T}{1+\gamma T}$. Then by (2.18) we obtain that for certain constant $c_\beta > 0$,

$$\|E^N\|^2_{T,\omega} \le c_\beta T^2N^{4-2r}\int_0^T \omega^{r-\frac{3}{2}}(t)\Big(\frac{d^r}{dt^r}U(t)\Big)^2dt. \tag{2.55}$$

The above with (2.39) gives that

$$\begin{aligned}\|U - u^N\|^2_{T,\omega} &\le 2\|U - \mathcal{I}_{T,N}U\|^2_{T,\omega} + 2\|\mathcal{I}_{T,N}U - u^N\|^2_{T,\omega}\\ &\le cN^{-2r}\int_0^T \omega^{r-\frac{1}{2}}(t)\Big(\frac{d^r}{dt^r}U(t)\Big)^2dt + c_\beta T^2N^{4-2r}\int_0^T \omega^{r-\frac{3}{2}}(t)\Big(\frac{d^r}{dt^r}U(t)\Big)^2dt\\ &\le c_\beta T^2N^{4-2r}\int_0^T \omega^{r-\frac{3}{2}}(t)\Big(\frac{d^r}{dt^r}U(t)\Big)^2dt.\end{aligned} \tag{2.56}$$

In particular,

$$\int_0^T \Big(U(t)-u^N(t)\Big)^2 dt \le \frac{T}{2}\int_0^T \Big(U(t)-u^N(t)\Big)^2 \omega^{-\frac{1}{2}}(t)dt = \frac{T}{2}\|U-u^N\|^2_{T,\omega}. \tag{2.57}$$

A combination of the previous two inequalities leads to (2.44). It remains to estimate (2.45). Clearly,

$$|U(T)-u^N(T)|^2 \le 2|U(T)-\mathcal{I}_{T,N}U(T)|^2 + 2|\mathcal{I}_{T,N}U(T)-u^N(T)|^2. \tag{2.58}$$

According to (2.52), we have

$$|U(T)-\mathcal{I}_{T,N}U(T)|^2 \le \frac{\pi}{4}\Big(\|U-\mathcal{I}_{T,N}U\|^2_{T,\omega} + T^2\|\frac{d}{dt}(U-\mathcal{I}_{T,N}U)\|^2_{T,\omega}\Big). \tag{2.59}$$

The above with (2.39) and (2.40) gives that

$$|U(T)-\mathcal{I}_{T,N}U(T)|^2 \le cT^2N^{4-2r}\int_0^T \omega^{r-\frac{3}{2}}(t)\Big(\frac{d^r}{dt^r}U(t)\Big)^2 dt. \tag{2.60}$$

We next estimate $|\mathcal{I}_{T,N}U(T)-u^N(T)|^2$. By (2.52) we obtain that

$$\begin{aligned}|\mathcal{I}_{T,N}U(T)-u^N(T)|^2 &\le \frac{\pi}{4}\Big(\|\mathcal{I}_{T,N}U-u^N\|^2_{T,\omega} + T^2\|\frac{d}{dt}(\mathcal{I}_{T,N}U-u^N)\|^2_{T,\omega}\Big)\\ &= \frac{\pi}{4}\Big(\|E^N\|^2_{T,\omega} + T^2\|\frac{d}{dt}E^N\|^2_{T,\omega}\Big).\end{aligned} \tag{2.61}$$

Moreover, by (2.9) and (2.32) we derive that

$$\begin{aligned}\|\frac{d}{dt}E^N\|^2_{T,\omega} &= (\frac{d}{dt}E^N,\frac{d}{dt}E^N)_{T,N} = \Big(G^N_{T,1}+G^N_{T,2},\frac{d}{dt}E^N\Big)_{T,N}\\ &\le \Big(\|G^N_{T,1}\|_{T,N}+\|G^N_{T,2}\|_{T,N}\Big)\|\frac{d}{dt}E^N\|_{T,N}\\ &= \Big(\|G^N_{T,1}\|_{T,\omega}+\|G^N_{T,2}\|_{T,N}\Big)\|\frac{d}{dt}E^N\|_{T,\omega},\end{aligned} \tag{2.62}$$

or equivalently,

$$\|\frac{d}{dt}E^N\|_{T,\omega} \le \|G^N_{T,1}\|_{T,\omega}+\|G^N_{T,2}\|_{T,N}. \tag{2.63}$$

Substituting (2.42), (2.46) and (2.55) into (2.63), we get that

$$\begin{aligned}\Big\|\frac{d}{dt}E^N\Big\|^2_{T,\omega} &\le cN^{4-2r}\int_0^T \omega^{r-\frac{3}{2}}(t)\Big(\frac{d^r}{dt^r}U(t)\Big)^2 dt\\ &\quad + c_\beta\gamma^2T^2N^{4-2r}\int_0^T \omega^{r-\frac{3}{2}}(t)\Big(\frac{d^r}{dt^r}U(t)\Big)^2 dt.\end{aligned} \tag{2.64}$$

Since $0<\gamma T\le\beta<\frac{1}{4}$, we have from (2.61), (2.64) and (2.55) that

$$|\mathcal{I}_{T,N}U(T)-u^N(T)|^2 \le c_\beta T^2N^{4-2r}\int_0^T \omega^{r-\frac{3}{2}}(t)\Big(\frac{d^r}{dt^r}U(t)\Big)^2 dt. \tag{2.65}$$

Finally, a combination of (2.58), (2.60) and (2.65) leads to

$$|U(T)-u^N(T)|^2 \le c_\beta T^2N^{4-2r}\int_0^T \omega^{r-\frac{3}{2}}(t)\Big(\frac{d^r}{dt^r}U(t)\Big)^2 dt. \tag{2.66}$$

This leads to (2.45). □

2.4. Numerical results

In this subsection, we present some numerical results to illustrate the efficiency of the aforementioned single interval algorithm. Throughout this paper, we take, for simplicity, the initial guess of the numerical solutions at the collocation points to be a zero vector.

Consider the following problem:

$$\begin{cases} \dfrac{d}{dt}U(t) = \exp\left(\frac{1}{5}\sin\left(U(t)\right)\right) + f(t), & 0 < t \le T, \\ U(0) = 1, \end{cases} \tag{2.67}$$

where

$$f(t) = \frac{3}{2}(t+1)^{\frac{1}{2}} + 10\cos 2t - \exp\left(\frac{1}{5}\sin((t+1)^{\frac{3}{2}} + 5\sin 2t)\right). \tag{2.68}$$

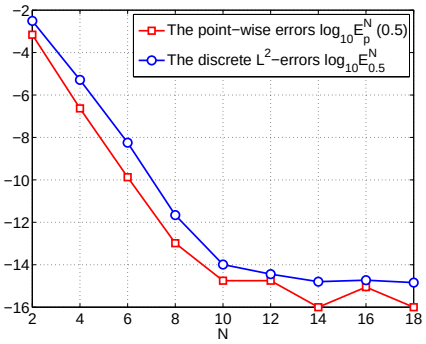

Fig. 2.1. The point-wise absolute errors and the discrete L^2-errors at $T = 0.5$.

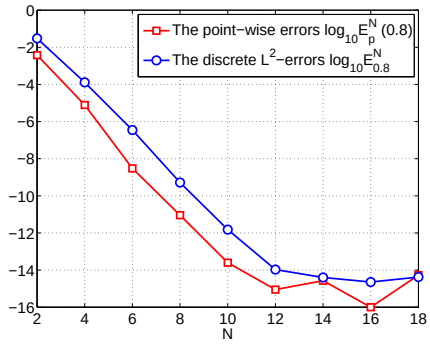

Fig. 2.2. The point-wise absolute errors and the discrete L^2-errors at $T = 0.8$.

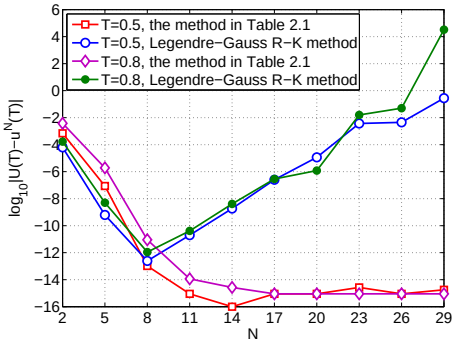

Fig. 2.3. The simple iterative algorithm vs. the $N+1$ stage implicit Legendre-Gauss Runge-Kutta method at $T = 0.5,\ 0.8$.

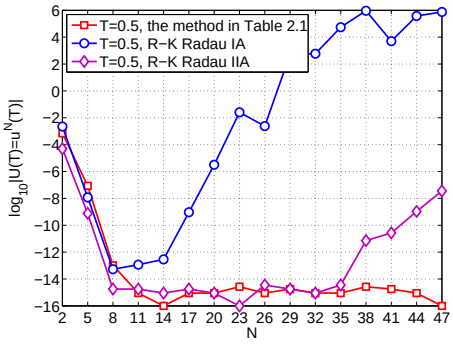

Fig. 2.4. The simple iterative algorithm vs. the $N+1$ stage implicit Legendre-Gauss-Radau Runge-Kutta methods at $T = 0.5$.

The exact solution of (2.67) is given by $U(t) = (t+1)^{\frac{3}{2}} + 5\sin 2t$, which oscillates and grows to infinity as $t \to \infty$. Eq. (2.67) fulfills the Lipschitz condition (2.17) with $\gamma = \frac{1}{5}\exp(\frac{1}{5})$. Therefore, as predicted by (2.44) and (2.45), for any $T < \frac{1}{4\gamma} = \frac{5}{4}\exp(-\frac{1}{5})$, the point-wise absolute errors $|U(T) - u^N(T)|$ and the $L^2(0,T)-$errors decay exponentially as $N \to \infty$.

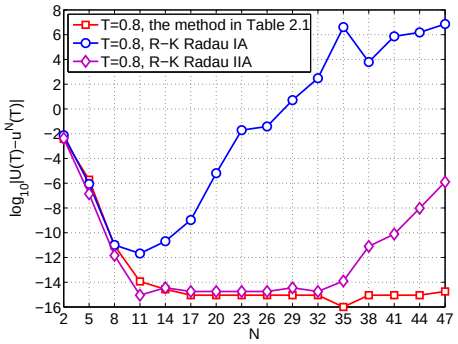

Fig. 2.5. The simple iterative algorithm vs. the $N+1$ stage implicit Legendre-Gauss-Radau Runge-Kutta methods at $T = 0.8$.

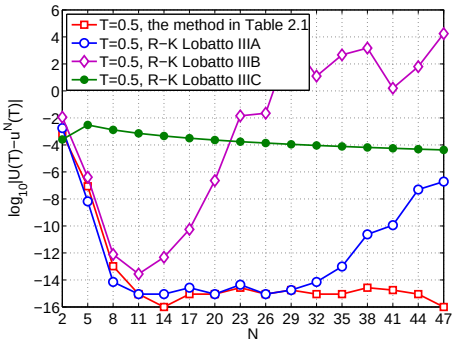

Fig. 2.6. The simple iterative algorithm vs. the $N+1$ stage implicit Legendre-Gauss-Lobatto Runge-Kutta methods at $T = 0.5$.

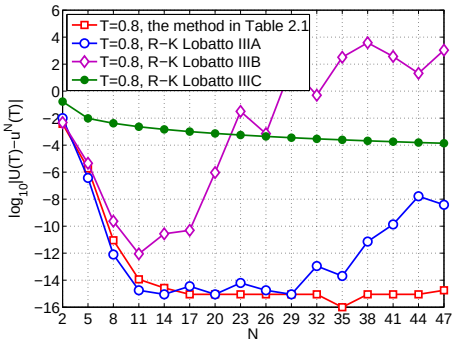

Fig. 2.7. The simple iterative algorithm vs. the $N+1$ stage implicit Legendre-Gauss-Lobatto Runge-Kutta methods at $T = 0.8$.

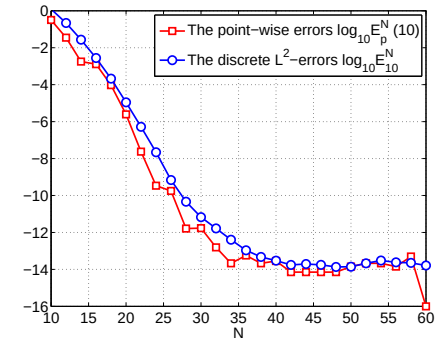

Fig. 2.8. The point-wise absolute errors and the discrete L^2-errors at $T = 10$.

We use the simple iterative algorithm described in Table 2.1 of Subsection 2.2 to resolve the problem (2.67). For description of numerical errors, we denote by $E_p^N(T)$ and E_T^N the point-wise absolute errors and the discrete L^2-errors, respectively, i.e.,

$$E_p^N(T) = |U(T) - u^N(T)|, \qquad E_T^N = \|U - u^N\|_{T,N}.$$

In Figs. 2.1 and 2.2, we plot the point-wise absolute errors $\log_{10} E_p^N(T)$ and the discrete L^2-errors $\log_{10} E_T^N$ at $T = 0.5,\ 0.8$ with various values of N. Clearly, the numerical errors decay exponentially as N increases. This coincides very well with theoretical analysis.

In Fig. 2.3, we compare the simple iterative algorithm described in Table (2.1) with the $N+1$ stage implicit Legendre-Gauss Runge-Kutta method. In Figs. 2.4 and 2.5, we compare the simple iterative algorithm with the $N+1$ stage implicit Legendre-Gauss-Radau Runge-Kutta methods (Radau IA and Radau IIA) as presented in [1, 10, 13, 24, 29] at $T = 0.5,\ 0.8$, respectively. In Figs. 2.6 and 2.7, we compare the simple iterative algorithm with the $N+1$ stage implicit Legendre-Gauss-Lobatto Runge-Kutta methods (Lobatto IIIA, Lobatto IIIB and Lobatto IIIC) as presented in [1, 10, 13, 24, 29] at $T = 0.5,\ 0.8$, respectively. We find that the simple iterative algorithm is accurate and stable. We also see the instability of some high-order Runge-Kutta methods.

It is pointed out that our algorithms often work very well even for large T. In Fig. 2.8, we

plot the point-wise absolute errors $\log_{10} E_p^N(T)$ and the discrete L^2-errors $\log_{10} E_T^N$ at $T = 10$ with various values of N, using the simple iterative algorithm. Clearly, the numerical errors decay exponentially as N increases. However, if we use Legendre-Gauss-type Runge-Kutta methods with $T = 10$, the numerical solution will not converge to the correct value.

3. A Multi-interval Chebyshev-Gauss Collocation method

In the previous section, we investigated the single interval Chebyshev-Gauss collocation method. The numerical errors decay very rapidly as N and r increase. However, in actual computation, it is not effective to resolve (2.16) with very large mode N. On the other hand, for ensuring the convergence of scheme (2.16), the length of T is limited sometimes, such as the condition (2.18). To remedy these deficiencies, it is advisable to partition the interval $(0, T)$ into a finite number of subintervals and solve the equations subsequently on each subinterval, using the suggested algorithms in Subsection 2.2 with moderate mode N. This technique simplifies computation, saves work, and still keeps the spectral accuracy. Moreover, it also provides us sufficient flexibility to adapt to the evolutionary process of solutions, e.g., we may use geometrically refined steps and linearly increasing degree vectors to resolve the singular behavior of the solution.

3.1. The multi-interval scheme

Let M be any positive integer and $\tau = \frac{T}{M}$. Replacing T by τ in (2.16) and all formulas in Section 2, we can derive an alternative algorithm, with which we obtain the numerical solution $u_1^N(t)$ for $0 \le t \le \tau$. In particular, $u_1^N(0) = U_0$. Next, we evaluate the numerical solutions $u_m^N(t) \in \mathcal{P}_{N+1}(0, \tau)$, $2 \le m \le M$, such that

$$\begin{cases} \dfrac{d}{dt} u_m^N(t_{\tau,k}^N) = f(u_m^N(t_{\tau,k}^N), m\tau - \tau + t_{\tau,k}^N), & 0 \le k \le N, \ \ 2 \le m \le M, \\ u_m^N(0) = u_{m-1}^N(\tau), & 2 \le m \le M. \end{cases} \tag{3.1}$$

Finally, the global numerical solution of (2.16) is given by

$$u^N(t + m\tau - \tau) = u_m^N(t), \qquad 0 \le t \le \tau, \qquad 1 \le m \le M. \tag{3.2}$$

According to Proposition 2.1, the method (3.1) also admits a unique solution, provided that $0 < \gamma\tau \le \beta < \frac{1}{4}$.

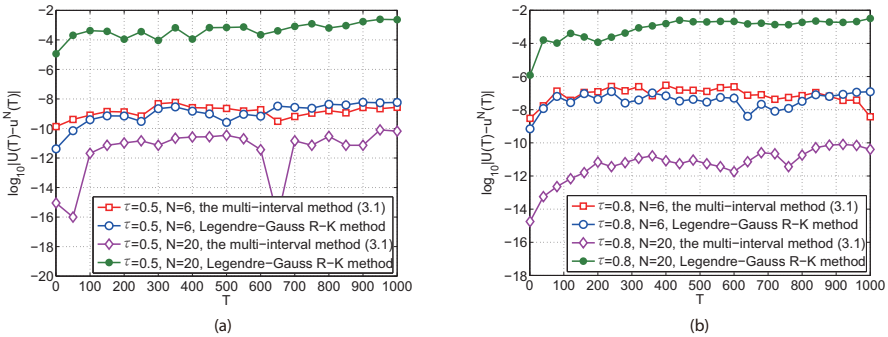

Fig. 3.1. The multi-interval method (3.1) vs. the $N + 1$ stage implicit Legendre-Gauss Runge-Kutta method with (a) $\tau = 0.5$ and (b) $\tau = 0.8$.

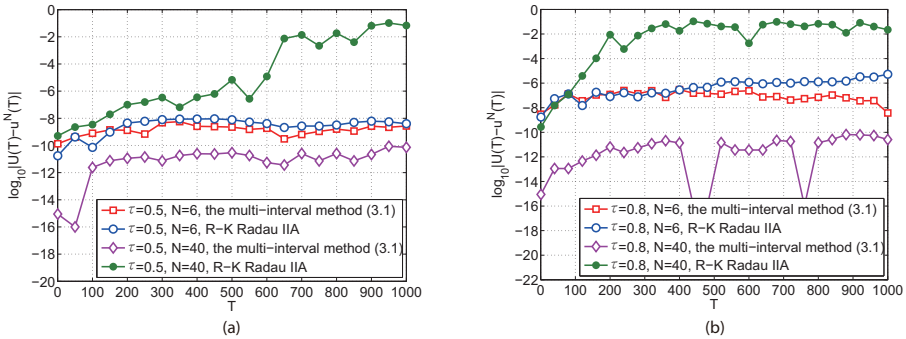

Fig. 3.2. The multi-interval method (3.1) vs. the $N+1$ stage implicit Legendre-Gauss-Radau IIA Runge-Kutta method with (a) $\tau = 0.5$ and (b) $\tau = 0.8$.

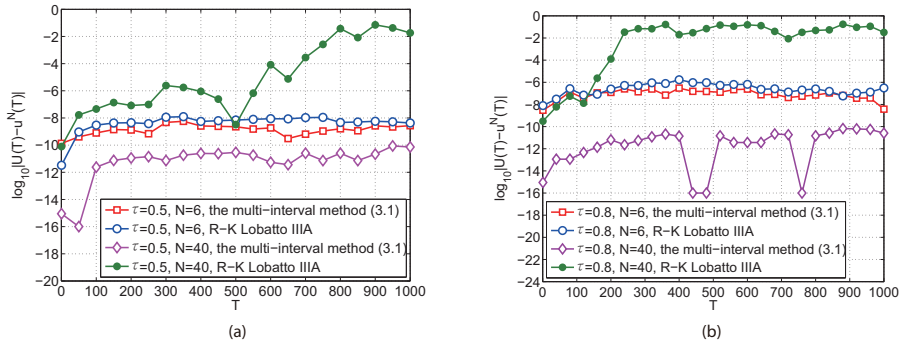

Fig. 3.3. The multi-interval method (3.1) vs. the $N+1$ stage implicit Legendre-Gauss-Lobatto IIIA Runge-Kutta method with (a) $\tau = 0.5$ and (b) $\tau = 0.8$.

3.2. Numerical results

In this subsection, we present some numerical results to illustrate the efficiency of the multi-interval method.

3.2.1. Nonlinear problems

We first consider the problem (2.67), and resolve it numerically, using the multi-interval scheme (3.1), combined with the simple iterative algorithm described in Table 2.1 of Subsection 2.2 at each time step.

In Fig. 3.1, we compare the multi-interval method (3.1) with the usual $N+1$ stage implicit Legendre-Gauss Runge-Kutta method, by taking $\tau = 0.5,\ 0.8$ and $N = 6,\ 20$, respectively. In Fig. 3.2, we compare the multi-interval method (3.1) with the usual $N+1$ stage implicit Legendre-Gauss-Radau IIA Runge-Kutta method, by taking $\tau = 0.5,\ 0.8$ and $N = 6,\ 40$, respectively. In Fig. 3.3, we compare the multi-interval method (3.1) with the usual $N+1$ stage implicit Legendre-Gauss-Lobatto IIIA Runge-Kutta method, by taking $\tau = 0.5,\ 0.8$ and $N = 6,\ 40$, respectively. We find that our method provides more accurate numerical results, especially for large N.

We next consider another nonlinear problem (cf. [26]):

$$\begin{cases} y'(t) = -\epsilon^{-1}(y^3(t) - g^3(t)) + g'(t), & t \in (0, T], \\ y(0) = 1, \end{cases} \tag{3.3}$$

with $g(t) = \cos(t)$ and the exact solution given by $y(t) = \cos(t)$.

Denoted by $y^N(t)$ the global numerical solutions, and Err the maximum of the absolute errors:

$$Err = \max_j |y(j\tau) - y^N(j\tau)|. \tag{3.4}$$

We use the multi-interval scheme (3.1) to resolve (3.3) numerically. In Figs. 3.4, we plot the absolute errors Err of this algorithm, by using the Newton iterative method (NIM) and the simple iterative method (SIM) with $\epsilon = 1$ and $T = 1000$. In Table 3.1, we list the CPU time consumption between NIM and SIM. We observe that the simple iterative method takes less computation time (due to lower cost at each iteration) and achieves the same level of accuracy. But the convergence behaviors of two iterative methods are different. In Fig. 3.5, we also take $\epsilon = 10^{-3}$ and plot the absolute errors at $T = 1$, using the Newton iterative method. Clearly, the numerical errors decay exponentially as N increases. However, in this case the simple iterative method does not converge to the solution.

Table 3.1: The comparison of CPU time consumption between NIM and SIM.

	$\tau = 1$		$\tau = 0.5$		$\tau = 0.1$		$\tau = 0.05$	
N	NIM	SIM	NIM	SIM	NIM	SIM	NIM	SIM
2	8.72	3.52	17.56	7.58	87.60	37.46	175.92	74.70
3	14.10	3.94	28.80	8.98	141.01	43.67	287.81	88.02
4	21.65	4.55	44.03	10.15	218.03	50.52	411.71	101.77
5	31.38	5.48	64.92	11.43	316.88	56.27	595.71	115.08
6	43.27	5.77	89.89	13.68	434.30	63.68		
7	58.39	6.49	117.92	14.05	585.12	70.48		
8	75.72	6.91	153.91	15.76				
9	96.56	7.47	195.55	16.97				
10	121.69	8.09						

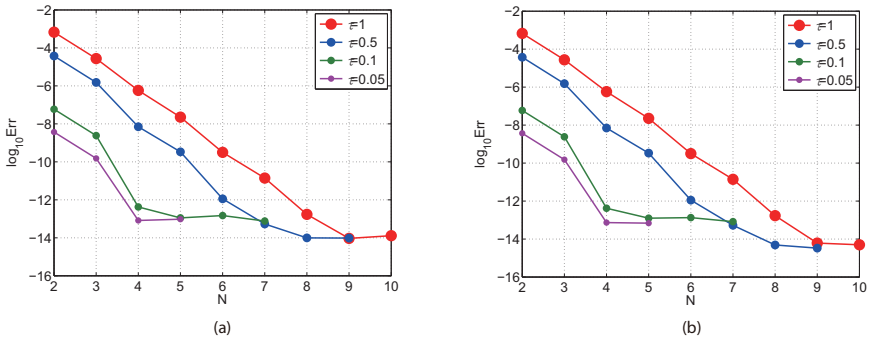

Fig. 3.4. The maximum of the absolute errors of (3.3) by (a) the Newton iterative method and (b) the simple iterative method with $\epsilon = 1$ and $T = 1000$.

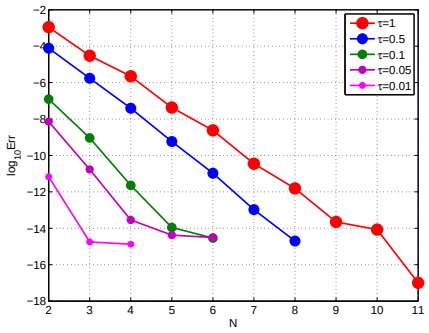

Fig. 3.5. The maximum of the absolute errors of (3.3) by the Newton iterative method with $\epsilon = 10^{-3}$ and $T = 1$.

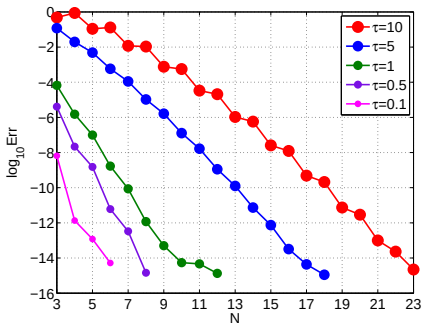

Fig. 3.6. The maximum of the absolute errors of scheme (3.6) with moderate τ and N.

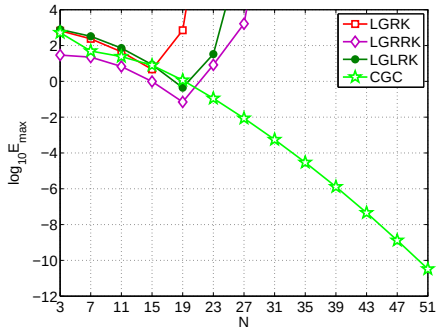

Fig. 3.7. Numerical errors of (3.10) with $a = b = 1$ and $\tau = 0.1$.

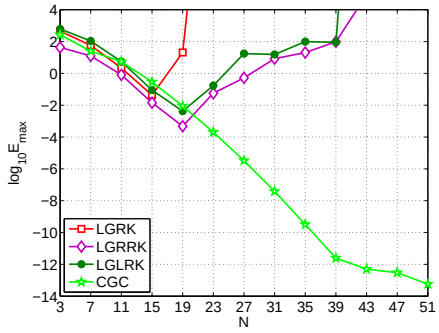

Fig. 3.8. Numerical errors of (3.10) with $a = b = 1$ and $\tau = 0.05$.

3.2.2. Stiff problems

We consider two linear stiff problems in this subsection. The first one is the Prothero-Robinson equation (cf. [33]):

$$\begin{cases} y'(t) = \lambda(y(t) - g(t)) + g'(t), & t \in [0, 10], \\ y(0) = 0, \end{cases} \tag{3.5}$$

with $\lambda = -10^6$, $g(t) = \sin(t)$ and the exact solution given by $y(t) = \sin(t)$.

We use the multi-interval scheme (3.1) to resolve (3.5) numerically. At each time step, we use the algorithm described in Subsection 2.2. More precisely, we use the following scheme:

$$\begin{aligned} &\frac{d}{dt} y_m^N(t_{\tau,k}^N) = \lambda\Big(y_m^N(t_{\tau,k}^N) - g(m\tau - \tau + t_{\tau,k}^N)\Big) \\ &\qquad\qquad + g'(m\tau - \tau + t_{\tau,k}^N), \qquad 0 \le k \le N,\ 1 \le m \le M, \\ &y_m^N(0) = y_{m-1}^N(\tau), \qquad 2 \le m \le M, \\ &y_1^N(0) = 0, \end{aligned} \tag{3.6}$$

where $\tau = \frac{10}{M}$, and $y_m^N(t)$ is the numerical solutions of $y(t)$ at the interval $(m\tau - \tau, m\tau)$.

For clarity, we next describe the numerical implementation. Let

$$y_m^N(t) = \sum_{j=0}^{N+1} \widehat{y}_j^m \mathcal{T}_{\tau,j}(t), \qquad \forall\ t \in (0,\tau). \tag{3.7}$$

Then, by (2.13) and (2.14) we get

$$\mathcal{I}_{\tau,N} y_m^N(t) = \sum_{j=0}^{N} \widehat{y}_j^m \mathcal{T}_{\tau,j}(t).$$

Hence, by (2.24) we obtain that

$$\begin{aligned} &\widehat{y}_{N+1}^m = \frac{\tau}{4(N+1)}(\lambda \widehat{y}_N^m - \lambda a_N^m + b_N^m), \qquad \widehat{y}_N^m = \frac{\tau}{4N}(\lambda \widehat{y}_{N-1}^m - \lambda a_{N-1}^m + b_{N-1}^m), \\ &\widehat{y}_j^m = \frac{\tau}{4j}\Big(c_{j-1}(\lambda \widehat{y}_{j-1}^m - \lambda a_{j-1}^m + b_{j-1}^m) - (\lambda \widehat{y}_{j+1}^m - \lambda a_{j+1}^m + b_{j+1}^m)\Big), \quad 1 \le j \le N-1, \end{aligned} \tag{3.8}$$

where a_j^m and b_j^m are the expansion coefficients of $\mathcal{I}_{\tau,N} g(m\tau - \tau + t)$ and $\mathcal{I}_{\tau,N} g'(m\tau - \tau + t)$, respectively. Due to (3.7), we have

$$y_m^N(0) = \sum_{j=0}^{N+1} (-1)^j \widehat{y}_j^m, \quad \Longrightarrow \quad \widehat{y}_0^m = y_m^N(0) - \sum_{j=1}^{N+1} (-1)^j \widehat{y}_j^m. \tag{3.9}$$

From (3.8) and (3.9), we further derive a system of $N+1$ linear algebraic equations in $N+1$ unknowns $\{\widehat{y}_j^m\}_{j=1}^{N+1}$, which can be solved efficiently.

Next denoted by $y^N(t)$ the global numerical solutions, and Err the maximum of the absolute errors as in (3.4).

In Fig. 3.6, we present the absolute errors Err of this algorithm, with moderate τ and N. They show that for stiff problem (3.5), our method provides accurate numerical results.

We next consider another stiff system (cf. [29]):

$$\begin{cases} \dfrac{d}{dt}P(t) = -2P(t) + Q(t) + 2\sin t, & 0 < t \le 1, \\ \dfrac{d}{dt}Q(t) = 998P(t) - 999Q(t) + 999(\cos t - \sin t), & 0 < t \le 1. \end{cases} \tag{3.10}$$

The eigenvalues of coefficient matrix are $\lambda_1 = -1000$ and $\lambda_2 = -1$. It is easy to verify that

$$P(t) = ae^{-t} + be^{-1000t} + \sin t, \qquad Q(t) = ae^{-t} - 998be^{-1000t} + \cos t, \tag{3.11}$$

where a and b are arbitrary real numbers.

We use the multi-interval scheme (3.1) to resolve (3.10) numerically. For convenience, we introduce some notations:

- CGC: The multi-interval Chebyshev-Gauss collocation scheme (3.1), combined with the algorithm in Subsection 2.2 at each time step, (also cf. (3.8) for a similar process);
- LGRK: $N+1$ stage Legendre-Gauss Runge-Kutta method;
- LGRRK: $N+1$ stage Legendre-Gauss-Radau IIA Runge-Kutta method;
- LGLRK: $N+1$ stage Legendre-Gauss-Lobatto IIIA Runge-Kutta method.

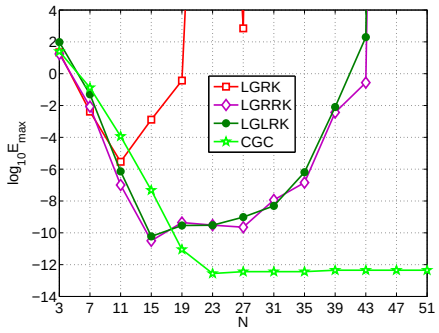

Fig. 3.9. Numerical errors of (3.10) with $a = b = 1$ and $\tau = 0.01$.

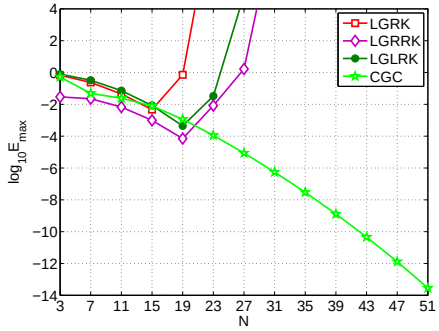

Fig. 3.10. Numerical errors of (3.10) with $a = -\frac{1}{999}$, $b = \frac{1}{999}$ and $\tau = 0.1$.

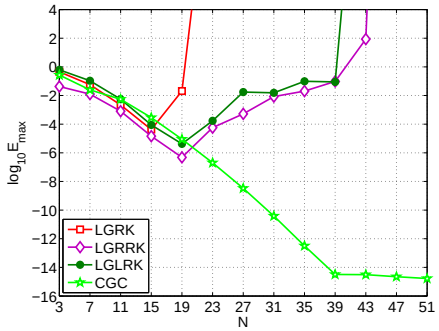

Fig. 3.11. Numerical errors of (3.10) with $a = -\frac{1}{999}$, $b = \frac{1}{999}$ and $\tau = 0.05$.

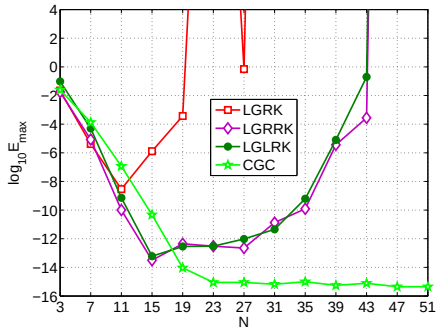

Fig. 3.12. Numerical errors of (3.10) with $a = -\frac{1}{999}$, $b = \frac{1}{999}$ and $\tau = 0.01$.

Let M be a positive integer and $\tau = \frac{1}{M}$. Denoted by $p^N(t)$ and $q^N(t)$ the global numerical solutions. We measure the numerical errors by the maximum norm:

$$E_{\max} = \max_{1\le j\le M} \Big(|P(j\tau) - p^N(j\tau)|, |Q(j\tau) - q^N(j\tau)| \Big).$$

In Figs. 3.7-3.9, we plot the values of $\log_{10} E_{\max}$ of our methods (CGC) and various $N+1$ stage Runge-Kutta methods for problem (3.10) with $a = b = 1$ and $\tau = 0.1,\ 0.05,\ 0.01$, respectively.

In Figs. 3.10-3.12, we also plot the values of $\log_{10} E_{\max}$ of our methods and various $N+1$ stage Runge-Kutta methods for problem (3.10) with $a = -\frac{1}{999}$, $b = \frac{1}{999}$ and $\tau = 0.1,\ 0.05,\ 0.01$, respectively.

We observe again that for stiff system (3.10), the multi-interval scheme (3.1) also provides more accurate and stable numerical results, especially for large τ and N.

3.2.3. Oscillating solution

We consider the second order ODE (cf. [32]):

$$\begin{cases} y''(t) + \lambda^2 y(t) = a\sin(\lambda t), \quad 0 < t \le 1, \\ y(0) = 1, \\ y'(0) = -\frac{a}{2\lambda}. \end{cases} \tag{3.12}$$

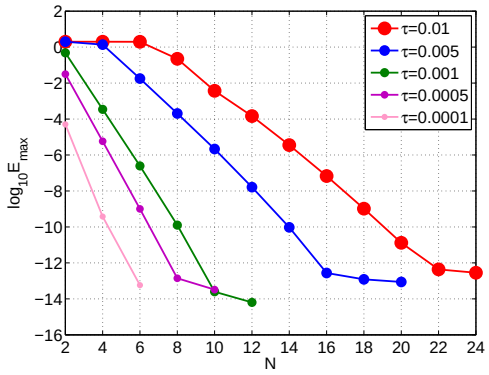

Fig. 3.13. The numerical errors of problem (3.13) with moderate τ and N.

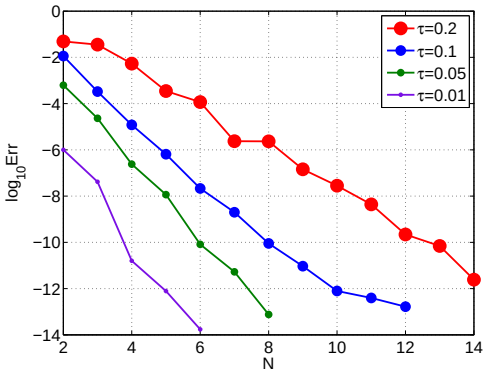

Fig. 3.14. The maximum of the absolute errors of problem (3.15) with moderate τ and N.

It can be converted to a system of the first order equations

$$\begin{cases} y_1'(t) = \lambda y_2(t), & 0 < t \le 1, \\ y_2'(t) = -\lambda y_1(t) + \frac{a}{\lambda}\sin(\lambda t), & 0 < t \le 1, \\ y_1(0) = 1, \\ y_2(0) = -\frac{a}{2\lambda^2}. \end{cases} \tag{3.13}$$

The exact solutions are

$$\begin{cases} y_1(t) = (1 - \frac{at}{2\lambda})\cos(\lambda t), \\ y_2(t) = -(1 - \frac{at}{2\lambda})\sin(\lambda t) - \frac{a}{2\lambda^2}\cos(\lambda t). \end{cases} \tag{3.14}$$

We take $a = 100$ and $\lambda = 1000$ as in [32]. Clearly, the solutions are highly oscillating. We resolve (3.13) using the multi-interval scheme (3.1). In Fig. 3.13, we plot the numerical errors $E_{\max}$ of this algorithm, with moderate τ and N. They indicate that our algorithm is very effective for highly oscillating solutions. It is noted that Petzold [32] also provided some numerical results with the error of order $10^{-3} \sim 10^{-5}$.

3.2.4. Steep gradient solution

We consider the nonlinear ODE:

$$\begin{aligned} U'(t) =& \frac{U(t)}{U^2(t)+1} + (-100t + 500)\exp(-50(t-5)^2) \\ & - \frac{\exp(-50(t-5)^2)}{\exp(-100(t-5)^2)+1}, \quad t \in [0, 10]. \end{aligned} \tag{3.15}$$

The exact solution $U(t) = \exp(-50(t-5)^2)$ is a Gaussian function, which has extremely steep gradients near $t = 5$.

We resolve (3.15) numerically using the multi-interval scheme (3.1), combined with the simple iterative algorithm described in Table 2.1. In Fig. 3.14, we plot the absolute errors Err of this algorithm, with moderate τ and N. They indicate that our algorithm is also valid even for steep gradient solutions.

3.2.5. Long time calculation

We consider the simple hamiltonian system:

$$\begin{cases} P'(t) = -4Q(t), & 0 < t \le T, \\ Q'(t) = P(t), & 0 < t \le T, \\ P(0) = 1, \quad Q(0) = 0. \end{cases} \tag{3.16}$$

Obviously, $P(t) = \cos(2t)$ and $Q(t) = \frac{1}{2}\sin(2t)$.

We resolve (3.16) using the multi-interval scheme (3.1). More precisely, we use the following scheme:

$$\begin{cases} \dfrac{d}{dt}p_m^N(t_{\tau,k}^N) = -4q_m^N(t_{\tau,k}^N), & 0 \le k \le N, \quad 1 \le m \le M, \\ \dfrac{d}{dt}q_m^N(t_{\tau,k}^N) = p_m^N(t_{\tau,k}^N), & 0 \le k \le N, \quad 1 \le m \le M, \\ p_m^N(0) = p_{m-1}^N(\tau), \quad q_m^N(0) = q_{m-1}^N(\tau), & 2 \le m \le M, \\ p_1^N(0) = 1, \quad q_1^N(0) = 0, \end{cases} \tag{3.17}$$

where $\tau = \frac{T}{M}$, and $p_m^N(t)$ and $q_m^N(t)$ are the numerical solutions of $P(t)$ and $Q(t)$ at the interval $(m\tau - \tau, m\tau)$.

For clarity, we describe the numerical implementation. Let

$$p_m^N(t) = \sum_{j=0}^{N+1} \widehat{p}_j^m \mathcal{T}_{\tau,j}(t), \qquad q_m^N(t) = \sum_{j=0}^{N+1} \widehat{q}_j^m \mathcal{T}_{\tau,j}(t), \qquad \forall\ t \in (0,\tau). \tag{3.18}$$

Then, by (2.13) and (2.14) we get that

$$\mathcal{I}_{\tau,N} p_m^N(t) = \sum_{j=0}^{N} \widehat{p}_j^m \mathcal{T}_{\tau,j}(t), \qquad \mathcal{I}_{\tau,N} q_m^N(t) = \sum_{j=0}^{N} \widehat{q}_j^m \mathcal{T}_{\tau,j}(t).$$

Hence, by (2.24) we obtain that

$$\begin{cases} \widehat{p}_{N+1}^m = -\dfrac{\tau \widehat{q}_N^m}{N+1}, & \widehat{p}_N^m = -\dfrac{\tau \widehat{q}_{N-1}^m}{N}, & \widehat{p}_j^m = -\dfrac{\tau(c_{j-1}\widehat{q}_{j-1}^m - \widehat{q}_{j+1}^m)}{j}, & 1 \le j \le N-1, \\ \widehat{q}_{N+1}^m = \dfrac{\tau \widehat{p}_N^m}{4(N+1)}, & \widehat{q}_N^m = \dfrac{\tau \widehat{p}_{N-1}^m}{4N}, & \widehat{q}_j^m = \dfrac{\tau(c_{j-1}\widehat{p}_{j-1}^m - \widehat{p}_{j+1}^m)}{4j}, & 1 \le j \le N-1. \end{cases} \tag{3.19}$$

Due to (3.18), we have

$$p_m^N(0) = \sum_{j=0}^{N+1} (-1)^j \widehat{p}_j^m, \qquad q_m^N(0) = \sum_{j=0}^{N+1} (-1)^j \widehat{q}_j^m. \tag{3.20}$$

Thus, by eliminating the variables $\widehat{p}_j^m,\ 0 \le j \le N+1$ and $\widehat{q}_0^m$ in (3.19), we derive that

$$\begin{cases} (1+\frac{5}{8}\tau^2)\widehat{q}_1^m - \frac{4}{3}\tau^2\widehat{q}_2^m + \frac{\tau^2}{8}\widehat{q}_3^m + \tau^2\sum_{j=3}^{N}(-1)^{j+1}\frac{j^2}{j^2-1}\widehat{q}_j^m + (-1)^N\tau^2\widehat{q}_{N+1}^m \\ = \frac{\tau}{2}p_m^N(0) - \tau^2 q_m^N(0), \\ \frac{\tau^2}{4}\sum_{j=1}^{N+1}(-1)^{j+1}\widehat{q}_j^m + (1-\frac{\tau^2}{6})\widehat{q}_2^m + \frac{\tau^2}{24}\widehat{q}_4^m = -\frac{\tau^2}{4}q_m^N(0), \\ \frac{\tau^2}{4j(j-1)}\widehat{q}_{j-2}^m + (1-\frac{\tau^2}{2(j^2-1)})\widehat{q}_j^m + \frac{\tau^2}{4j(j+1)}\widehat{q}_{j+2}^m = 0, \qquad 3 \le j \le N-2, \\ \frac{\tau^2}{4(N-1)(N-2)}\widehat{q}_{N-3}^m + (1-\frac{\tau^2}{2N(N-2)})\widehat{q}_{N-1}^m = 0, \\ \frac{\tau^2}{4N(N-1)}\widehat{q}_{N-2}^m + (1-\frac{\tau^2}{4N(N-1)})\widehat{q}_N^m = 0, \\ \frac{\tau^2}{4N(N+1)}\widehat{q}_{N-1}^m + \widehat{q}_{N+1}^m = 0. \end{cases} \tag{3.21}$$

In actual computation, we first compute the coefficients $\{\widehat{q}_j^m\}_{j=1}^{N+1}$ by (3.21), and then compute the coefficients $\widehat{q}_0^m$ and $\{\widehat{p}_j^m\}_{j=0}^{N+1}$ by (3.20) and (3.19).

Next let $p^N(t)$ and $q^N(t)$ be the global numerical solutions of $P(t)$ and $Q(t)$, and denote the point-wise absolute error by

$$E^N(t) = \sqrt{|p^N(t) - P(t)|^2 + |q^N(t) - Q(t)|^2}.$$

For convenience, we also introduce some notations:

- CGC: Chebyshev-Gauss collocation method presented in this subsection;
- LGC: Legendre-Gauss collocation method presented in [18];
- LGRC: Legendre-Gauss-Radau collocation method presented in [45];
- LGLC: Legendre-Gauss-Lobatto collocation method presented in [19].

In Tables 3.2 and 3.3, we list the point-wise errors $E^N(t)$ and the corresponding CPU time (CPUT) of various numerical methods at $t = 10^7$, with moderate τ and N. They show that our method costs less computational time and provides more accurate and stable numerical results.

4. Concluding Discussions

In this paper, we proposed the single interval and multi-interval Chebyshev-Gauss collocation methods for ODEs. We also suggested two algorithms, which can be implemented efficiently. These approaches have several fascinating features:

- The single interval Chebyshev-Gauss collocation method is easy to implement, and enjoys computational efficiency, accuracy and stability over some popular numerical approaches.

Table 3.2: Comparison of various numerical methods for problem (3.16).

		CGC		LGRK		LGRRK		LGLRK	
τ	N	$E^N(t)$	CPUT	$E^N(t)$	CPUT	$E^N(t)$	CPUT	$E^N(t)$	CPUT
0.1	7	6.62e-10	1.84e3	1.45e-7	1.65e3	1.27e-8	1.68e3	2.13e-9	1.65e3
0.25	9	2.19e-10	7.52e2	1.38e-5	7.12e2	9.13e-9	7.20e2	1.47e-8	6.86e2
0.5	11	7.00e-11	3.90e2	2.36e-4	3.64e2	5.16e-9	3.70e2	1.50e-9	3.49e2
1	13	2.89e-10	2.00e2	6.46e-2	1.89e2	1.66e-9	1.97e2	5.00e-9	1.82e2
2	16	7.31e-10	1.03e2	7.51e-1	1.00e2	3.81e-9	1.04e2	2.61e-9	95.82
4	21	1.70e-9	55.31	7.51e-1	6.59e2	1.17e-7	1.02e2	1.09e-7	97.38
8	33	1.83e-10	41.47	–	–	7.36e-2	1.86e2	1.18e-1	1.78e2
16	44	1.35e-9	24.40	–	–	–	–	–	–
32	70	4.64e-10	16.26	–	–	–	–	–	–

Table 3.3: Comparison of various numerical methods for problem (3.16).

		CGC		LGC		LGRC		LGLC	
τ	N	$E^N(t)$	CPUT	$E^N(t)$	CPUT	$E^N(t)$	CPUT	$E^N(t)$	CPUT
0.1	7	6.62e-10	1.84e3	2.73e-8	2.83e3	1.28e-6	2.58e3	2.53e-6	2.37e3
0.25	9	2.19e-10	7.52e2	1.68e-8	1.21e3	2.87e-7	1.17e3	1.94e-7	1.01e3
0.5	11	7.00e-11	3.90e2	1.32e-8	6.64e2	9.38e-8	6.26e2	1.51e-7	5.37e2
1	13	2.89e-10	2.00e2	2.25e-8	3.47e2	1.20e-7	3.33e2	1.85e-7	2..84e2
2	16	7.31e-10	1.03e2	1.58e-9	1.87e2	4.14e-7	1.78e2	3.41e-7	1.66e2
4	21	1.70e-9	55.31	2.31e-8	1.13e2	2.04e-7	1.05e2	1.60e-7	95.27
8	33	1.83e-10	41.47	2.32e-9	80.40	8.68e-8	77.38	1.70e-7	67.91
16	44	1.35e-9	24.40	1.71e-8	53.13	7.09e-8	50.30	3.07e-7	45.82
32	70	4.64e-10	16.26	1.44e-9	44.61	6.84e-8	42.02	1.09e-7	39.81

- The multi-interval Chebyshev-Gauss collocation method can not only help us to solve the resultant system more efficiently and economically, but also provide us sufficient flexibility to adapt to the evolutionary process of solutions. Moreover, the numerical results indicate that the convergence can be obtained by refining the time steps (h-method) and/or increasing the order of trial functions (p-method).

- The suggested approaches often work very well even for large step-size τ.

Numerical illustrations also show that the suggested algorithms are particularly attractive for ODEs with stiff behaviors, oscillating solutions, steep gradient solutions and long time calculations.

Appendix

A. *Proof of Proposition 2.1.*

As usual, we consider the following iteration process:

$$\begin{cases} \dfrac{d}{dt}u^{N,m}(t_{T,k}^N) = f(u^{N,m-1}(t_{T,k}^N), t_{T,k}^N), & 0 \le k \le N, \quad m \ge 1, \\ u^{N,m}(0) = U_0, \qquad m \ge 0. \end{cases} \tag{4.1}$$

Denote $\widetilde{u}^{N,m}(t) = u^{N,m}(t) - u^{N,m-1}(t)$. Then we have from (4.1) that, for m$\geq$ 2,

$$\frac{d}{dt}\widetilde{u}^{N,m}(t_{T,k}^N) = f(u^{N,m-1}(t_{T,k}^N), t_{T,k}^N) - f(u^{N,m-2}(t_{T,k}^N), t_{T,k}^N), \qquad 0 \le k \le N. \tag{4.2}$$

In addition, $\widetilde{u}^{N,m}(0) = 0$.

We next show the contraction property of $\widetilde{u}^{N,m}(t)$. Obviously, by (2.33) we have

$$\frac{T}{2}\|t^{-1}\widetilde{u}^{N,m}\|^2_{T,\omega} \le 2((T-t)t^{-1}\widetilde{u}^{N,m}, \frac{d}{dt}\widetilde{u}^{N,m})_{T,N}. \tag{4.3}$$

On the other hand, by (4.2), (2.17), (2.9) and (2.15), we get that

$$\begin{aligned} 2((T-t)t^{-1}\widetilde{u}^{N,m}, \frac{d}{dt}\widetilde{u}^{N,m})_{T,N} &\le 2\gamma\|(T-t)t^{-1}\widetilde{u}^{N,m}\|_{T,N}\|\widetilde{u}^{N,m-1}\|_{T,N} \\ \le 2\gamma T\|t^{-1}\widetilde{u}^{N,m}\|_{T,N}\|\widetilde{u}^{N,m-1}\|_{T,N} &\le 2\gamma T\|t^{-1}\widetilde{u}^{N,m}\|_{T,\omega}\|\widetilde{u}^{N,m-1}\|_{T,\omega}. \end{aligned} \tag{4.4}$$

A combination of (4.3) and (4.3) leads to

$$\|\widetilde{u}^{N,m}\|_{T,\omega} \le T\|t^{-1}\widetilde{u}^{N,m}\|_{T,\omega} \le 4\gamma T\|\widetilde{u}^{N,m-1}\|_{T,\omega}.$$

It follows that, if $0 \le 4\gamma T \le \beta < 1$, then $\|\widetilde{u}^{N,m}\|_{T,\omega} \to 0$ as $m \to \infty$, and thus, the proof is complete.

B. *Proof of* (2.52).

For any $v \in H^1(0,T)$ and $0 \le t_1 \le t_2 \le T$, we have that

$$|v(t_2) - v(t_1)| \le \int_{t_1}^{t_2} |v'(t)|dt \le \Big(\int_0^T \sqrt{t(T-t)}dt \int_0^T \frac{|v'(t)|^2}{\sqrt{t(T-t)}}dt\Big)^{\frac{1}{2}} \le \frac{\sqrt{2\pi}T}{4}\|v'\|_{T,\omega}.$$

Next let $|v(t^*)| = \min\limits_{t\in[0,T]} |v(t)|$. Then, by the previous inequality, we get that

$$|v(t)| - |v(t^*)| \le |v(t) - v(t^*)| \le \frac{\sqrt{2\pi}T}{4}\|v'\|_{T,\omega}.$$

Moreover

$$|v(t^*)| \le \frac{1}{T}\int_0^T |v(t)|dt \le \frac{1}{T}\Big(\int_0^T \sqrt{t(T-t)}dt \int_0^T \frac{v^2(t)}{\sqrt{t(T-t)}}dt\Big)^{\frac{1}{2}} \le \frac{\sqrt{2\pi}}{4}\|v\|_{T,\omega}.$$

Therefore

$$|v(t)| \le \frac{\sqrt{2\pi}}{4}\Big(\|v\|_{T,\omega} + T\|v'\|_{T,\omega}\Big).$$

Acknowledgments. The authors would like to thank the anonymous referees for their helpful suggestions and comments to improve the manuscript. The work of Wang Zhong-qing (corresponding author) was supported by NSF of China, No. 11171225, the Research Fund for Doctoral Program of Higher Education of China, No. 20133127110006, Innovation Program of Shanghai Municipal Education Commission, No. 12ZZ131, and the Fund for E-institute of Shanghai Universities, No. E03004.

References

[1] O. Axelsson, A class of A-stable methods, *BIT*, **9** (1969), 185-199.

[2] P.Z. Bar-Yoseph, D. Fisher and O. Gottlieb, Spectral element methods for nonlinear spatio-temporal dynamics of an Euler-Bernoulli beam, *Comput. Mech.,* **19** (1996), 136-151.

[3] P.Z. Bar-Yoseph and E. Moses, Space-time spectral element methods for unsteady convection-diffusion problems, *Int. J. Numer. Methods for Heat & Fluid Flow,* **7** (1997), 215-235.
[4] C. Bernardi and Y. Maday, Spectral method, in Handbook of Numerical Analysis, part 5, edited by P.G. Ciarlet and J.L. Lions, North-Holland, 1997.
[5] J.P. Boyd, Chebyshev and Fourier Spectral Methods, Springer-Verlag, Berlin, 1989.
[6] J.C. Butcher, Implicit Runge-Kutta processes, *Math. Comp.,* **18** (1964), 50-64.
[7] J.C. Butcher, Integration processes based on Radau quadrature formulas, *Math. Comp.,* **18** (1964), 233-244.
[8] J.C. Butcher, The Numerical Analysis of Ordinary Differential Equations, Runge-Kutta and General Linear Methods, John wiley & Sons, Chichester, 1987.
[9] C. Canuto, M.Y. Hussaini, A. Quarteroni and T.A. Zang, Spectral Methods: Fundamentals in single domains, Springer-Verlag, Berlin, 2006.
[10] F.H. Chipman, A-stable Runge-Kutta processes, *BIT*, **11** (1971), 384-388.
[11] P. Dutt, Spectral methods for initial-boundary value problems-an alternative approach, *SIAM J. Numer. Anal.,* **27** (1990), 885-903.
[12] Feng Kang, Difference schemes for Hamiltonian formulism and symplectic geometry, *J. Comput. Math.,* **4** (1986), 279-289.
[13] K. Feng and M. Qin, Sympletic Geometric Algorithms for Hamiltonian Systems, Zhejiang Science and Technology Press, Hangzhou, 2003.
[14] D. Funaro, Polynomial Approximations of Differential Equations, Springer-Verlag, 1992.
[15] D. Gottlieb and S.A. Orszag, Numerical Analysis of Spectral Methods: Theory and Applications, SIAM-CBMS, Philadelphia, 1977.
[16] B. Guo, Spectral Methods and Their Applications, World Scientific, Singapore, 1998.
[17] B. Guo and L. Wang, Jacobi approximations in non-uniformly Jacobi-weighted Sobolev spaces, *J. Approx. Theory,* **128** (2004), 1-41.
[18] B. Guo and Z. Wang, Legendre-Gauss collocation methods for ordinary differential equations, *Adv. Comput. Math.,* **30** (2009), 249-280.
[19] B. Guo and Z. Wang, A spectral collocation method for solving initial value problems of first order ordinary differential equations, *Discrete Contin. Dyn. Syst. Ser. B*, **14** (2010), 1029-1054.
[20] B. Guo and Z. Wang, Numerical integration based on Laguerre-Gauss interpolation, *Comput. Methods Appl. Mech. Engrg.*, **196** (2007), 3726-3741.
[21] B. Guo, Z. Wang, H. Tian and L. Wang, Integration processes of ordinarny differential equations based on Laguerre-Radau interpolations, *Math. Comp.*, **77** (2008), 181-199.
[22] E. Hairer, C. Lubich and G. Wanner, Geometric Numerical Integration: Structure-Preserving Algorithms for Ordinary Differential Equations, Springer Series in Comput. Mathematics, Vol. 31, Springer-Verlag, Berlin, 2002.
[23] E. Hairer, S. P. Norsett and G. Wanner, Solving Ordinary Differential Equation I: Nonstiff Problems, Springer-Verlag, Berlin, 1987.
[24] E. Hairer and G. Wanner, Solving Ordinary Differential Equation Ⅱ: Stiff and Differential – Algebraic Problems, Springer-Verlag, Berlin, 1991.
[25] D.J. Higham, Analysis of the Enright-Kamel partitioning method for stiff ordinary differential equations, *IMA J. Numer. Anal.*, **9** (1989), 1-14.
[26] P.J. van der Houwen and B.P. Sommeijer, Iterated Runge-Kutta methods on parallel computers, *SIAM J. Sci. Statist. Comput.*, **12** (1991), 1000-1028.
[27] G. Ierley, B. Spencer and R. Worthing, Spectral methods in time for a class of parabolic partial differential equations, *J. Comput. Phys.,* **102** (1992), 88-97.
[28] N. Kanyamee and Z. Zhang, Comparison of a spectral collocation method and symplectic methods for Hamiltonian systems, *Int. J. Numer. Anal. Model.*, **8** (2011), 86-104.
[29] J.D. Lambert, Numerical Methods for Ordinary Differential Systems, The Initial Value Problem, John Wiley and Sons, Chichester, 1991.

[30] D.L. Lewis, John Lund and Kenneth L. Bowers, The space-time sinc-Galerkin method for parabolic problems, *Int. J. Numer. Methods Engrg.,* **24** (1987), 1629-1644.

[31] Bart De Maerschalck and Marc I. Gerritsma, The use of Chebyshev polynomials in the space-time least-squares spectral element method, *Numer. Algorithms,* **38** (2005), 173-196.

[32] L.R. Petzold, An efficient numerical method for highly oscillatory ordinary differential equations, *SIAM J. Numer. Anal.,* **18** (1981), 455-479.

[33] A. Prothero and A. Robinson, On the stability and the accuracy of one-step methods for solving stiff systems of ordinary differential equations, *Math. Comput.*, **28** (1974), 145-162.

[34] H. Ramos and R. García-Rubio, Analysis of a Chebyshev-based backward differentiation formulae and relation with Runge-Kutta collocation methods, *Int. J. Comput. Math.*, **88** (2011), 555-577.

[35] H. Ramos and J. Vigo-Aguiar, An almost L-stable BDF-type method for the numerical solution of stiff ODEs arising from the method of lines, *Numer. Methods Partial Differential Equations*, **23** (2007), 1110-1121.

[36] J.M. Sanz-Serna and M.P. Calvo, Numerical Hamiltonian Problems, AMMC7, Chapman and Hall, London, 1994.

[37] J. Shen and T. Tang, Spectral and High-order Methods With Applications, Science Press, Beijing, 2006.

[38] J. Shen, T. Tang and L. Wang, Spectral Methods: Algorithms, Analysis and Applications, Springer Series in Computational Mathematics, Vol. 41, 2011.

[39] A.M. Stuart and A.R. Humphries, Dynamical systems and Numerical Analysis, Cambridge University Press, Cambridge, 1996.

[40] H. Tal-Ezer, Spectral methods in time for hyperbolic equations, *SIAM J. Numer. Anal.*, **23** (1986), 11-26.

[41] H. Tal-Ezer, Spectral methods in time for parabolic problems, *SIAM J. Numer. Anal.*, **26** (1989), 1-11.

[42] J. Tang and H. Ma, Single and multi-interval Legendre τ-methods in time for parabolic equations, *Adv. Comput. Math.*, **17** (2002), 349-367.

[43] J. Tang and H. Ma, A Legendre spectral method in time for first-order hyperbolic equations, *Appl. Numer. Math.*, **57** (2007), 1-11.

[44] J. Vigo-Aguiar and H. Ramos, A family of A-stable Runge-Kutta collocation method of higher order for initial-value problems, *IMA J. Numer. Anal.*, **27** (2007), 798-817.

[45] Z. Wang and B. Guo, Legendre-Gauss-Radau collocation method for solving initial value problems of first order ordinary differential equations, *J. Sci. Comput.*, **52** (2012), 226-255.

[46] Thomas P. Wihler, An a priori error analysis of the *hp*-version of the continuous Galerkin FEM for nonlinear initial value problems, *J. Sci. Comput.*, **25** (2005), 523-549.